Journal of Hydrology 498 (2013) 254–264

Contents lists available at SciVerse ScienceDirect

Journal of Hydrology

journal homepage: www.elsevier.com/locate/jhydrol

Hillslope scale temporal stability of soil water storage in diverse soil layers

Xiaoxu Jia [a], Ming'an Shao [a,b,*], Xiaorong Wei [a], Yunqiang Wang [a,c]

[a] State Key Laboratory of Soil Erosion and Dryland Farming on the Loess Plateau, Northwest A&F University, Yangling 712100, China
[b] Institute of Soil and Water Conservation, Northwest A&F University, Yangling 712100, China
[c] State Key Laboratory of Loess and Quaternary Geology, Institute of Earth Environment, Chinese Academy of Sciences, Xi'an, Shaanxi 710075, China

ARTICLE INFO

Article history:
Received 28 February 2013
Received in revised form 16 April 2013
Accepted 25 May 2013
Available online 21 June 2013
This manuscript was handled by
Konstantine P. Georgakakos, Editor-in-Chief

Keywords:
Soil water storage
Temporal stability
Representative location
Hillslope hydrology
The Loess Plateau

SUMMARY

Knowledge of the soil water storage (SWS) of soil profiles on the scale of a hillslope is important for the optimal management of soil water and revegetation on sloping land in semi-arid areas. This study aimed to investigate the temporal stability of SWS profiles (0–1.0, 1.0–2.0, and 2.0–3.0 m) and to identify representative sites for reliably estimating the mean SWS on two adjacent hillslopes of the Loess Plateau in China. We used two indices: the standard deviation of relative difference (SDRD) and the mean absolute bias error (MABE). We also endeavored to identify any correlations between temporal stability and soil, topography, or properties of the vegetation. The SWS of the soil layers was measured using neutron probes on 15 occasions at 59 locations arranged on two hillslopes (31 and 28 locations for hillslope A (HA) and hillslope B (HB), respectively) from 2009 to 2011.

The time-averaged mean SWS for the three layers differed significantly ($P < 0.05$) between HA and HB and was greatly affected by topography and vegetation. Temporal–spatial analyses showed that the temporal variation of SWS decreased with increasing soil depth, while the spatial variation increased on both hillslopes. Comparisons of the values for SDRD and MABE and the number of time-stable locations with SDRD and MABE < 5% among various depths indicated that temporal stability increased with an increase in soil depth. The representative sites identified for each hillslope (two on HA and one on HB) accurately estimated the mean SWS for the three soil layers ($R^2 \geqslant 0.95$, $P < 0.001$). SWS on the scale of a hillslope was strongly time stable, and the temporal–spatial patterns of SWS were highly dependent on sampling depth. The temporal stability of SWS patterns was controlled by soil texture, organic carbon content, elevation, and properties of the vegetation in the study area, which was characterised by diverse or complex terrains and plant cover. Such effects, however, might vary across hillslopes due to different conditions of wetness and patterns of land use. This study provides useful information on the profiles of mean SWS on the scale of a hillslope, which is necessary for improving the management of soil water on sloping land on the Loess Plateau.

1. Introduction

Soil water storage (SWS) of soil profiles is critical for understanding a number of hydrological and biological processes (Western et al., 2004; Choi and Jacobs, 2007; Brocca et al., 2009). It is also an important parameter for the rational management of water resources and adoption of vegetational restorations, especially in semi-arid and arid areas, such as the Loess Plateau in China (Hu et al., 2009, 2010a; Gao et al., 2011). Soil moisture is variable in space and time due to soil heterogeneity, climatic forcing, vegetation and topography, but it also shows a somewhat strong temporal stability of spatial pattern (Vachaud et al., 1985; Comegna and Basile, 1994; Mohanty and Skaggs, 2001; Martínez-Fernández and Ceballos, 2005; Brocca et al., 2009, 2010; Hu et al., 2009; Zhao et al., 2010). The concept of temporal stability was first proposed by Vachaud et al. (1985) and is defined as the time-invariant association between spatial location and classical statistical parameters of a given soil property. Kachanoski and de Jong (1988) later expanded the definition of the stability of soil moisture over time as a description of the temporal persistence of spatial pattern. One of the most useful applications of the concept of temporal stability is the potential to identify representative locations that could rapidly and effectively represent the mean SWS of the entire study area of interest. Various studies have recently confirmed and

* Corresponding author at: Institute of Soil and Water Conservation, Northwest A&F University, Yangling 712100, China. Fax: +86 29 87012210.
E-mail address: mashao@ms.iswc.ac.cn (M. Shao).

0022-1694/$ - see front matter © 2013 Elsevier B.V. All rights reserved.
http://dx.doi.org/10.1016/j.jhydrol.2013.05.042

supported this application of temporal stability (Gómez-Plaza et al., 2000; Grayson et al., 2002; Cosh et al., 2008; Hu et al., 2009; Zhao et al., 2010; Brocca et al., 2012).

The concept of temporal stability has been broadly applied in various types of land uses, such as grassland (Vachaud et al., 1985; Schneider et al., 2008; Zhao et al., 2010), cropland (Martínez-Fernández and Ceballos, 2003; Guber et al., 2008), and forests (Lin, 2006), and over different climatic zones, such as semi-arid (Gómez-Plaza et al., 2000; Hu et al., 2010a; Zhao et al., 2010), semi-humid (Brocca et al., 2009, 2010; Heathman et al., 2009), and humid (Jacobs et al., 2004) zones. This concept has also been applied to the study of soil moisture on the Loess Plateau, where the water content is the most crucial factor for the restoration of vegetation (Hu et al., 2009, 2010a,b; Gao et al., 2011; Gao and Shao, 2012; Jia and Shao, 2013). Most studies on the temporal stability of soil moisture on the Loess Plateau have focused on the surface soil layer, and only few of them (Hu et al., 2010b; Gao and Shao, 2012) have addressed the entire soil profile. The Loess Plateau is known for its complex terrains, patterns of land use, and soil types, which can lead to large spatial variations of soil water (Hu et al., 2009; Wang et al., 2012). Because the restoration of vegetation must be implemented on relatively small scales (e.g. hillslopes or small watersheds) due to the high variability of soil water, studies of the temporal stability of SWS for various soil layers on the scale of a hillslope can be very important for the optimal management of soil water on the Loess Plateau, especially during the restoration of vegetation (Hu et al., 2010a). Information characterising the temporal stability of the SWS profile on the scale of a hillslope is also helpful for developing more efficient and effective sampling strategies and predictive models for monitoring water in such areas with large variabilities of soil, terrain, and vegetation (Zhao et al., 2010).

The temporal stability of soil moisture has been linked to many factors, such as soil, topography, and vegetation. Elucidating the effects of various factors on the stability of SWS over time is beneficial both for the identification of representative locations and for projecting the temporal stability of areas that have not yet been sampled (Vanderlinden et al., 2011). These factors, however, contribute variously to the identification of representative locations of temporal stability of soil moisture due to differences in the landscapes, land uses, sampling scales, and sampling times. The temporal stability of soil water content in a watershed is mainly controlled by the distribution of soil particle size (Hu et al., 2010a). Gao et al. (2011) suggested that the best locations for estimating the mean soil moisture in sloping jujube orchards should be the locations with relatively high clay contents, relatively gentle slopes, and relatively planar surfaces, agreeing partly with the findings of Grayson and Western (1998) and Jacobs et al. (2004). Gómez-Plaza et al. (2000) identified topographic effects or local topography as the main influences on temporal stability of soil water content on the scale of a transect, as supported by a recent report (Penna et al., 2013) on the scale of hillslopes. The temporal persistence of soil moisture in a relatively flat semi-arid steppe depended on the management of grazing and on the related plant cover (Schneider et al., 2008). Temporal stability is also dependent on soil depth (Martínez-Fernández and Ceballos, 2003; Pachepsky et al., 2005; Guber et al., 2008; Hu et al., 2010b). Soil moisture in deeper layers tends to be more stable (Guber et al., 2008; Gao and Shao, 2012). Furthermore, the determination of the temporal stability of soil moisture can depend on the scale of the study (Kachanoski and de Jong, 1988; Gómez-Plaza et al., 2000; Biswas and Si, 2011). No consistent conclusions have thus been drawn on the factors contributing to temporal stability. In contrast to some studies with relatively uniform soil type, terrain, or vegetation, the relationships between the temporal stability of soil water and the potential contributing factors on the Loess Plateau may be complicated by the complex distribution of soil types, terrains, and plant covers.

Neutron probes have been widely used to measure soil water content (Caysi et al., 2009; Hu et al., 2009, 2010a, 2010b; Gao and Shao, 2012), because they can measure temporal changes at defined positions. Neutron probes yield accurate results (Muñoz-Carpena, 2012) and are non-destructive. They may be used irrespective of the state of the water. The output from neutron probes can be directly related to the soil water content (Chanasyk and Naeth, 1996). The equipment, however, requires extensive soil-specific calibration to obtain reliable data. Several studies have indicated that temporal stability of soil water may be affected by the type of sensor used (Kirda and Reichardt, 1992; Reichardt et al., 1997; Guber et al., 2008). The assessment of temporal stability of soil water using neutron probes, though, has been well demonstrated on the Loess Plateau (Hu et al., 2009, 2010a,b; Gao and Shao, 2012).

Because of the widespread restoration of vegetation on sloping land and the low carrying capacity of soil water for vegetation (Xia and Shao, 2008) in the study area, information on the SWS profiles on the scale of the hillslope is necessary to guide the strategies of revegetation and to optimise the management of water. For a deeper insight on the temporal stability of SWS profiles, this study used neutron probe data collected on two adjacent hillslopes, over 15 occasions from June 2009 to August 2011. The specific objectives of this study were: (i) to gain insight into the temporal–spatial characteristics of SWS for the various soil layers on two adjacent hillslopes, (ii) to analyse the temporal stability of SWS profiles for identifying representative locations that could estimate the mean SWS of a hillslope, and (iii) to investigate the factors that control the temporal stability of SWS profiles on the scale of a hillslope.

2. Materials and methods

2.1. Study site

This study was conducted on two typical hillslopes (HA and HB) of the Loess Plateau in the Liudaogou watershed located in Shenmu County, Shaanxi Province, China (Fig. 1). The Liudaogou watershed is characterised by many deep gullies and undulating loessial slopes. This area lies in a moderate-temperate and semiarid zone with an annual mean precipitation of 430 mm, approximately 77% of which occurs from July to September. The average annual temperature is 8.4 °C, and the mean annual potential evapotranspiration reaches 785 mm. The elevations of the Liudaogou watershed range from 1094 to 1274 m above sea level. The study area is representative of the transitional belt subjected to both wind and water erosion. The soil is a Calcaric Regosol (FAO-UNESCO), developed from low-fertility loess. The soil has weak cohesion, high infiltrability, low water retention, and is prone to erosion. The vegetation has been widely restored in the region during the past decade to remedy the degradation of the soil. This restoration used plants typical of arid land, including purple alfalfa (*Medicago sativa* L.), Korshinsk Peashrub (*Caragana korshinskii* K.), and apricot trees (*Prunus armeniaca*), or recovered abandoned cropland with natural vegetation.

The average slopes of HA and HB are approximately 14° and 19°, respectively. HA and HB are separated by a deep gully. The two hillslopes have received different strategies of vegetational restoration, which have created differences in the patterns of land use and thus in vegetational cover. Restored grassland and forest usually occur as patches in this area. The dominant land uses on HA are grassland occupied by bunge needlegrass (*Stipa bungeana* T.), with some alfalfa (*M. sativa* L.) and *Artemisia scoparia*, and forest with a low planting density of apricot trees. HA also contains some farmland for millet production. HB is mainly covered by abandoned

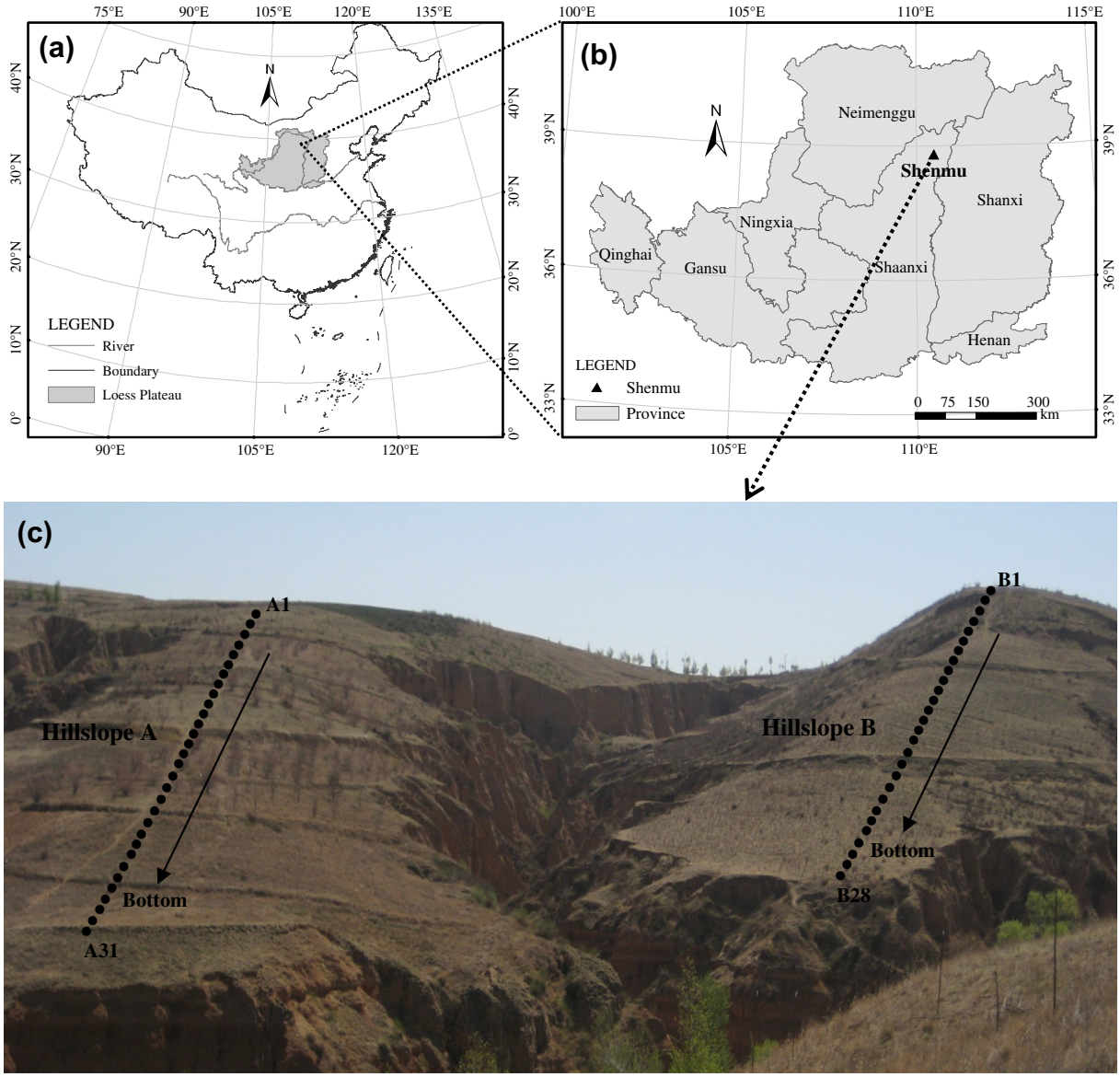

Fig. 1. Location of the study area and distribution of neutron access tubes on both hillslopes (from the top to the bottom of each slope, access tubes are marked as 1, 2,...,31, 31 and 28 sampling locations on HA and HB, respectively). Spaces between adjacent sampling locations are 10 m.

fields of alfalfa and bunge needlegrass and contains no trees or farmland. HA is thus relatively gentle sloped and has more complex patterns of land use and vegetational cover, while HB is relatively steep and has a more uniform land use. The distributions of daily rainfall and mean air temperatures at the study area from 2009 to 2011 are shown in Fig. 2.

2.2. Sampling and measurements

2.2.1. Measurement of soil water storage

Thirty-one (HA) and 28 (HB) aluminium neutron-probe access tubes, 3.2 m in length, were installed at regular intervals of approximately 10 m along a transect from the top to the bottom of (350 m) and HB (300 m) (Fig. 1). Soil water contents were measured using a neutron probe at these 59 neutron-probe locations during the growing seasons from June 1, 2009 to August 10, 2011. A total of 15 sampling occasions were recorded during the entire sampling period. Slow-neutron counts were taken at intervals of 0.2 m to a depth of 3.0 m. Volumetric soil water contents, θ, at each depth were calculated from the slow-neutron counting rates, CR, using the following calibration curve (Hu et al., 2009, 2010b):

$$\theta = 0.6483 \times CR - 0.0102 (R^2 = 0.90, P < 0.001) \quad (1)$$

The calibration curve was obtained for the same area and was considered valid for all depths. The SWS (mm) of the ith site at the jth time at the kth depth, SWS_{ijk}, was calculated from the θ_{ijk} (%, v/v) data (k refers to different soil depths, mm). The SWS of the 0–1.0, 1.0–2.0, and 2.0–3.0 m layers was calculated by the following trapezoidal rules, respectively:

$$SWS_{ij(0-1.0m)} = 200 \times [\theta_{ij(200)} + \theta_{ij(400)} + \theta_{ij(600)} + \theta_{ij(800)} + \theta_{ij(1000)}] \quad (2)$$

$$SWS_{ij(1.0-2.0m)} = 200 \times [\theta_{ij(1200)} + \theta_{ij(1400)} + \theta_{ij(1600)} + \theta_{ij(1800)} + \theta_{ij(2000)}] \quad (3)$$

$$SWS_{ij(2.0-3.0m)} = 200 \times [\theta_{ij(2200)} + \theta_{ij(2400)} + \theta_{ij(2600)} + \theta_{ij(2800)} + \theta_{ij(3000)}] \quad (4)$$

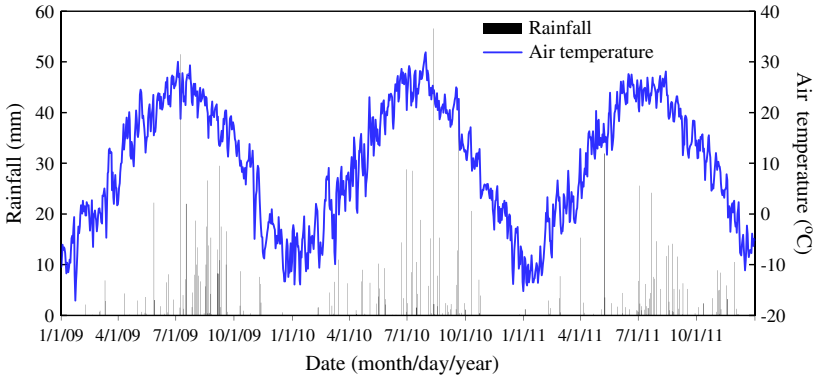

Fig. 2. Distribution of daily rainfall and mean air temperature at the study area from 2009 to 2011.

2.2.2. Measurement of other main characteristics

An RTK-GPS receiver was used to locate the sampling sites and record the corresponding elevations (above sea level) (SE, m). At each location, 0.5 m away from the access tube a 20 cm deep pit was excavated to take the undisturbed soil samples for measurements of saturated soil hydraulic conductivity (Ks, mm min^{-1}), using the constant-head method (Klute and Dirksen, 1986), and soil bulk density (BD, g cm^{-3}). Disturbed soil samples were also collected for laboratory analysis. The disturbed soil samples were air-dried and divided into two sub-samples. One sub-sample was passed through a 1 mm sieve and was analysed for soil particle sizes by laser diffraction using a Mastersizer2000 (Malvern Instruments, Malvern, England). The other sub-sample was passed through a 0.25 mm sieve to determine soil organic carbon (OC, g kg^{-1}) by dichromate oxidation method (Nelson and Sommers, 1982). In August 2011, we sampled peak aboveground biomass (AGB, g m^{-2}) of herbage on HB by clipping an area of 1 m × 1 m in each site. Litter fall (Litter, g m^{-2}) was also collected after aboveground plants were clipped. The plant samples were dried at 65 °C in an oven for 72 h to estimate dry weight. AGB and Litter data is not available on HA. The selected variables were taken to study the effects of soil, topography, and properties of vegetation on the temporal stability of SWS. The selected topsoil (0–20 cm), topography, and properties of the vegetation for the two hillslopes are listed in Table 1.

2.3. Assessment of the temporal stability of soil water storage

The effect of the temporal frequency of measurement on the determination of soil water temporal stability and the estimation of mean soil water content has only been researched to a small extent (Vanderlinden et al., 2011). Brocca et al. (2010) found that the sites of time-stable soil water identified from 12 sampling occasions (a total of 35 sampling occasions over 2 years) correctly represented the field means for more than 90% of cases. Gao et al. (2011) estimated the mean soil water contents of sloping jujube orchards reasonably well using temporal stability based on 16 of 28 sampling occasions. We thus deemed 15 sampling occasions to be sufficient for analysing the temporal stability of SWS and for identifying sites as being time stable.

Two methods were employed to assess the temporal stability of SWS. From Vachaud et al. (1985), the relative difference (RD) in SWS for the *i*th location at the *j*th time at the *k*th depth, δ_{ijk}, is calculated as:

$$\delta_{ijk} = \frac{SWS_{ijk} - \overline{SWS_{jk}}}{\overline{SWS_{jk}}} \quad (5)$$

where $\overline{SWS_{jk}}$ is the mean SWS of the hillslope at the *j*th time at the *k*th depth:

$$\overline{SWS_{jk}} = \frac{1}{M}\sum_{i=1}^{M} SWS_{ijk} \quad (6)$$

in which *M* is the number of sampling locations of the hillslope.

The temporal mean relative difference (MRD), $\overline{\delta_{ik}}$, and the associated standard deviation (SDRD) over time, $\sigma(\delta_{ik})$, are calculated as:

$$\overline{\delta_{ik}} = \frac{1}{N}\sum_{j=1}^{N} \delta_{ijk} \quad (7)$$

and

$$\sigma(\delta_{ik}) = \sqrt{\frac{1}{N-1}\sum_{j=1}^{N}(\delta_{ijk} - \overline{\delta_{ik}})^2} \quad (8)$$

where *N* is the total number of sampling occasions. The relative difference analysis mainly identifies the sites that systematically represent the mean SWS of the study area or over- or underestimate it while at the same time yielding a measure of variability (Vachaud et al., 1985; Mohanty and Skaggs, 2001). By this method, the time-stable locations tend to have MRDs close to zero and the minimum associated SDRD over time. According to Jacobs et al. (2004) and Zhao et al. (2010), an index of temporal stability (ITS) can be computed using a combination of MRD and the associated SDRD as follows:

$$ITS_{ik} = \sqrt{\overline{\delta_{ik}}^2 + \sigma(\delta_{ik})^2} \quad (9)$$

The ITS provides a single metric for identifying the sampling locations that are most representative of the mean hillslope SWS (i.e. low $\overline{\delta_{ik}}$) and are also temporally stable (i.e. low $\sigma(\delta_{ik})$). The

Table 1
Selected physical and chemical properties of topsoil (0–20 cm), site elevation (SE), and properties of the vegetation on HA and HB.

Variables	HA			HB		
	Mean	SD	CV (%)	Mean	SD	CV (%)
Clay, %	18.1	4.0	22.1	10.4	5.6	53.8
Silt, %	46.7	5.9	12.6	27.9	6.5	23.3
Sand, %	35.2	9.0	25.6	61.7	10.9	17.7
Ks, mm min^{-1}	0.6	0.3	50.0	0.3	0.2	66.7
BD, g cm^{-3}	1.2	0.1	8.3	1.4	0.1	7.1
OC, g kg^{-1}	4.0	0.9	22.5	3.5	1.9	54.3
SE, m	1187	14.0	1.2	1201	21	1.7
AGB, g m^{-2}	–	–	–	285.2	156.0	54.7
Litter, g m^{-2}	–	–	–	27.5	26.8	97.4

(a) SD, standard deviation; CV, coefficients of variation: (SD/M) * 100; Ks, saturated soil hydraulic conductivity; BD, bulk density; OC, organic carbon; and SE, site elevation.
(b) Aboveground biomass (AGB) and litter fall (Litter) data is not available on HA.

location with the highest temporal stability notably has the lowest ITS. An acceptable ITS threshold can be established to identify sites within a field that consistently represent the mean field SWS with a given accuracy (Zhao et al., 2010). In this study, sampling locations with an ITS under 10% were strictly selected as time-stable sites for each hillslope.

In the second method, mean absolute bias error (MABE), introduced by Hu et al. (2010b), was employed to determine time-invariant locations and to estimate error. According to Eq. (6), if δ_{ijk} and SWS_{ijk} are known a priori, then $\overline{sws_{jk}}$ can be calculated accurately as:

$$\overline{sws_{jk}} = \frac{SWS_{ijk}}{1+\delta_{ijk}} \tag{10}$$

Assuming a constant offset $\overline{\delta_{ik}}$ for a time-stable location (Grayson and Western, 1998), the estimated value of $\overline{sws_{jk}}$, $\overline{sws_{jk}}'$, can be expressed as:

$$\overline{sws_{jk}}' = \frac{SWS_{ijk}}{1+\overline{\delta_{ik}}} \tag{11}$$

Therefore, the estimate error of the mean SWS, φ_{ijk}, can be calculated as:

$$\varphi_{ijk} = \frac{\overline{sws_{jk}}' - \overline{sws_{jk}}}{\overline{sws_{jk}}} \tag{12}$$

Substituting $\overline{sws_{jk}}$ from Eq. (10) and $\overline{sws_{jk}}'$ from Eqs. (11) into (12), we have

$$\varphi_{jk} = \frac{\delta_{ijk} - \overline{\delta_{ik}}}{1+\overline{\delta_{ik}}} \tag{13}$$

The absolute value of φ_{jk}, $|\varphi_{jk}|$, can then be expressed as:

$$|\varphi_{jk}| = \left|\frac{\delta_{ijk} - \overline{\delta_{ik}}}{1+\overline{\delta_{ik}}}\right| \tag{14}$$

Therefore, the mean absolute value of bias error, $MABE_{ik}$, can be calculated as:

$$MABE_{ik} = \frac{1}{N}\sum_{j=1}^{N}\left|\frac{\delta_{ijk} - \overline{\delta_{ik}}}{1+\overline{\delta_{ik}}}\right| \tag{15}$$

where N is the total number of sampling occasions.$MABE_{ik}$ thus directly describes the time-averaged bias error from using the ith location to produce a mean SWS at the kth depth when consistently assuming the offset of $\overline{\delta_{ik}}$. Locations with lower values of MABE tend to be more temporally stable and to produce less estimate error. In this case, sampling locations with MABE lower than 5% were taken to be temporally stable (Hu et al., 2010b). Theoretically, if the pronounced representative locations identified by ITS coincided with the temporally stable sites identified by MABE, then the site should be the best for predicting the mean SWS of the study area of interest. In our study, we chose the time-stable locations with an ITS under 10% and a MABE under 5% to estimate mean SWS for the various soil layers on each hillslope.

3. Results and discussion

3.1. Temporal–spatial analysis of soil water storage for various soil layers

The temporal evolution of SWS for the various soil layers on both hillslopes is shown in Fig. 3a. The overall decrease in SWS at various depths during the study period was mainly caused by climatic factors and the uptake of soil water by roots. Precipitation from April to October (growing season) generally decreased over the 3 years, with the highest in 2009 (439.4 mm), followed by 2010 (394.1 mm). The lowest amount of precipitation from April to October was observed in 2011 (274.1 mm) (Fig. 2).

The values of time-averaged mean SWS for the various soil layers were significantly different between HA and HB. The time-averaged mean SWSs on HB were 30.2, 46.8, and 47.7 mm lower than those of HA for the 0–1.0, 1.0–2.0, and 2.0–3.0 m layers, respectively, which were significant ($P < 0.05$) by a paired-sample t-test (Table 2). Furthermore, the SWS in the 0–1.0 m soil layer on HB was typically higher than in deeper layers, while the mean SWS on HA was not significantly different among the three soil layers. These results can be attributed to differences in the characteristics of the plants on the two hillslopes, and specifically to the stronger evapotranspiration of alfalfa on HB. Alfalfa is a perennial deep-rooted plant that consumes much water by taking up soil water from deeper soil layers (Wang et al., 2010; Jia and Shao, 2013). The desiccation of soil caused by planting alfalfa, a common phenomenon on the Loess Plateau (Chen et al., 2008; Wang et al., 2010), may account for the significantly lower SWSs in deeper layers on HB than in shallower layers. Moreover, the relatively steep slope of HB can reduce the capacity for conserving the limited rainfall due to downslope drainage. HA was thus considered a relatively wet slope, while HB was considered a relatively dry slope.

Temporal changes in the hillslope-averaged SWS for the various soil layers (Fig. 3a) with the corresponding statistical parameters (Table 2) showed that the temporal changes in the mean SWS were highly dependent on sampling depth. The trends in the variation of mean SWS were largely similar on both hillslopes. The temporal changes in the mean SWS were mainly detected in the shallow layer (0–1.0 m), in agreement with the findings of Choi and Jacobs (2007), Hu et al. (2010b), Gao and Shao (2012), and Penna et al. (2013), who observed less variability in deeper than in shallower layers (Fig. 3a and Table 2). The standard deviations (SD_T) and coefficients of variation (CV_T) over time of the hillslope-averaged SWS at different soil depths also indicated that temporal changes in the mean SWS decreased with increasing soil depth on both hillslopes (Table 2). This association may be ascribed to the relatively higher variability caused by evaporation, rainfall, and/or absorption of soil water by roots in the shallower layer than the deeper layers. At deeper soil depths, the mean SWS underwent relatively small temporal changes. The temporal changes in standard deviations (SD_S) and coefficients of variation (CV_S) over space of mean SWS for both hillslopes indicated that SWS in deeper soil layers had greater spatial variability (Fig. 3b and c). Similar to the mean SWS, the larger temporal changes in spatial variability also tended to occur in the shallow layer (0–1.0 m), which had the highest values of SD_T and CV_T for the CV_S of SWS on both hillslopes (Table 2). This observation indicated that the mean SWS tended to be temporally more stable in deeper soil layers, in agreement with Lin (2006), Guber et al. (2008), Hu et al. (2010b), and Gao and Shao (2012).

3.2. Temporal stability of soil water storage for various soil layers

Fig. 4 presents the ranked MRD in SWS, the associated SDRD, and the ITS for each sampling location for the various soil layers on HA and HB. In general, the minimum, maximum, and ranges of MRD and SDRD for each soil layer were similar on both hillslopes (Table 3). These two variables, however, behaved differently among soil layers. The ranges between the minimum and maximum values of MRD were relatively larger in deeper soils on both hillslopes (Table 3). The increasing ranges of MRD might be ascribed to the stronger spatial variability of SWS with increasing soil depth (Fig. 3b and c). The observed ranges of MRD for the various soil layers on both hillslopes were inconsistent with the values observed in studies with smaller or larger scales of sampling (Vachaud et al., 1985; Mohanty and Skaggs, 2001; Martínez-Fernández and Ceballos, 2003; Schneider et al., 2008; Zhao et al., 2010). Schneider

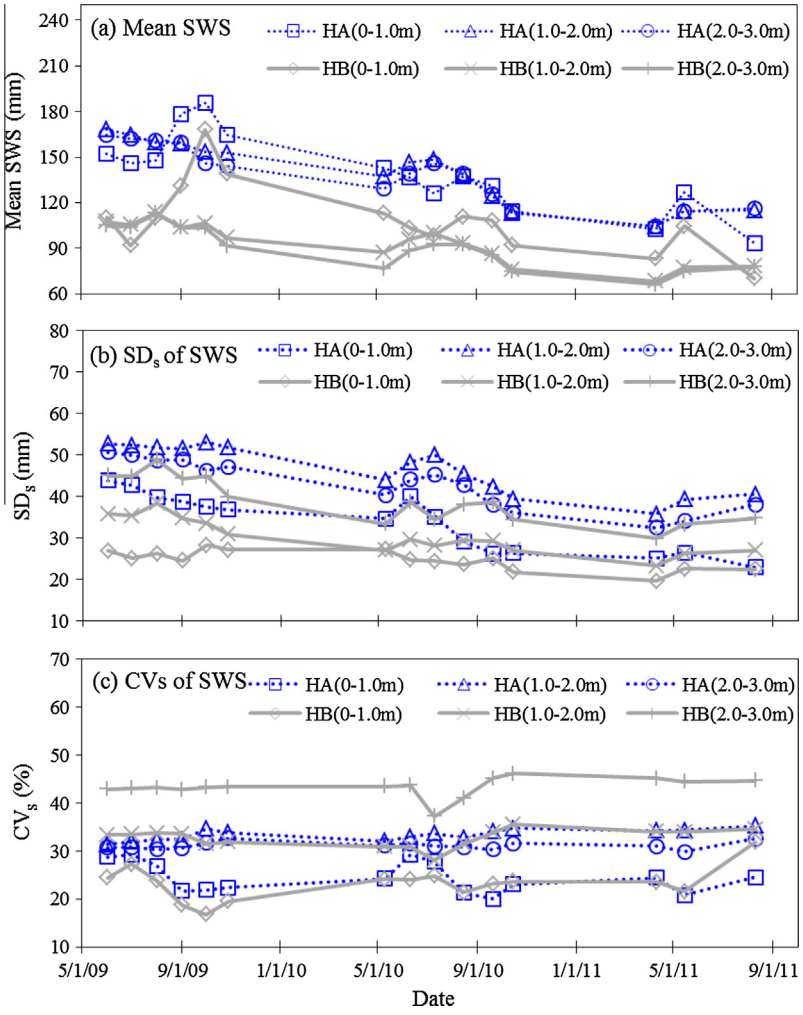

Fig. 3. Time series of spatial mean SWS and the associated standard deviation (SD_S) and coefficient of variation (CV_S) for the various soil layers on HA and HB.

Table 2
Temporal statistics (June 2009–August 2011) for spatial soil water storage (SWS) and the corresponding standard deviation (SD_S) and coefficients of variation (CV_S) for the various soil layers on HA and HB.

Spatial variables	Temporal statistics	HA			HB		
		0–1.0 m	1.0–2.0 m	2.0–3.0 m	0–1.0 m	1.0–2.0 m	2.0–3.0 m
Mean SWS	Mean, mm	139.2§a	140.1a	137.8a	109.0b	93.2c	90.1c
	Max, mm	185.5	168.1	164.9	168.3	113.6	112.9
	Min, mm	93.3	104.5	104.8	70.4	76.2	66.3
	SD_T, mm	25.4	20.8	19.6	23.6	13.6	13.9
	CV_T, %	18.3	14.9	14.2	21.7	14.6	15.5
SD_S of SWS	Mean, mm	33.7a	46.5b	42.8b	24.6c	30.4a	38.8d
	Max, mm	43.9	53.0	50.6	27.2	38.4	48.8
	Min, mm	22.9	35.7	32.5	19.6	23.3	29.9
	SD_T, mm	7.0	5.9	6.0	2.4	4.3	5.6
	CV_T, %	20.8	12.7	14.0	9.6	14.1	14.4
CV_S of SWS	Mean, %	24.4a	33.3c	31.1b	23.2a	32.7bc	43.3d
	Max, %	29.3	34.8	32.6	31.8	35.5	46.1
	Min, %	20.0	31.3	29.8	16.8	28.1	37.1
	SD_T, %	3.2	1.2	0.8	3.6	1.9	2.1
	CV_T, %	13.3	3.6	2.6	15.4	5.8	4.8

(a) SD_S of SWS is the standard deviation of the spatial SWS; CV_S of SWS is the coefficient of variation of the spatial SWS.
(b) Statistics in the second column are derived from the time series of statics in the first column. Thus, SD_T refers to the standard deviation of time series of the mean spatial SWS, SD_S of the spatial SWS, or CV_S of the spatial SWS; CV_T refers to the coefficient of variation of the time series of the mean spatial SWS, SD_S of the spatial SWS, or CV_S of the spatial SWS.
(c) § Means followed by the same lower letter are not significantly different at $P < 0.05$.

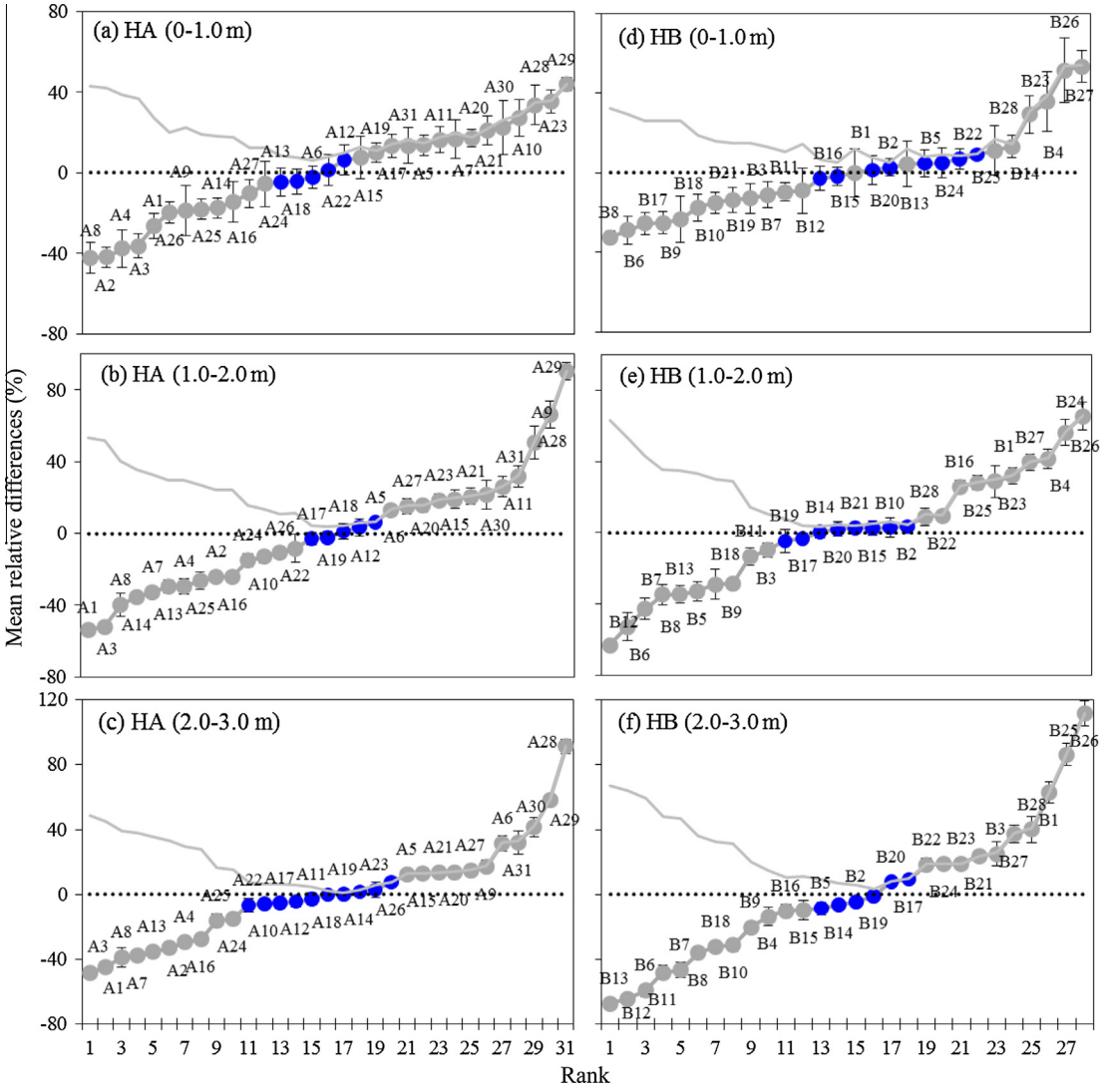

Fig. 4. Ranked mean relative differences of SWS and the index of time stability (ITS) for each sampling location on HA (a, b, and c) and HB (d, e, and f) for the various soil layers. Vertical bars represent ± one standard deviation of relative differences. The bold curve indicates the ITS, and the locations with ITS under 10% are marked in blue. (For interpretation of the references to colour in this figure legend, the reader is referred to the web version of this article.)

et al. (2008) and Brocca et al. (2009) showed that the range of MRD increases with the scale of sampling because of an expected increase in the variation of soils, topography, and vegetation. In the present study, though, a relatively larger range of MRD, especially at deeper soil depths, was observed at the smaller scale of the hillslope, which may be inconsistent with the conclusions by Schneider et al. (2008) and Brocca et al. (2009). This inconsistency may be partly due to the layout of the experiments, the measurement techniques, and the differences in soil, topography, and/or vegetation (Vanderlinden et al., 2011). For example, the wider range of soil textures (Hu et al., 2010a) or the strong topographic differences among sampling sites (Gómez-Plaza et al., 2000) may have led to a larger range of MRDs.

The mean values of SDRD generally decreased with increasing soil depth on both hillslopes, being 7.4%, 4.4%, and 3.3% for the 0–1.0, 1.0–2.0, and 2.0–3.0 m layers on HA, and 7.7%, 5.0%, and 4.2% for these layers on HB, respectively (Table 3). These results were in agreement with those of Hu et al. (2010a,b) and Gao and Shao (2012). If sites with SDRD and/or MABE values under 5% are taken to be temporally stable (Starks et al., 2006; Hu et al., 2010b), then the number of time-stable locations generally increased with increasing soil depth on both hillslopes. For example, the number of locations with SDRD or MABE < 5% was 5 or 11, respectively, for the 0–1.0 m layer on HA. For the 2.0–3.0 m soil layer, however, most of the sites were likely to be temporally stable because up to 28 or 29 sites were identified by SDRD or MABE, respectively (Table 3). We are thus tempted to conclude that the SWS in deeper soil layers tends to be more temporally stable due to the reduced dependence on the climatic, vegetational, and/or hydrological factors that influence the dynamics of soil moisture (Pachepsky et al., 2005; Vanderlinden et al., 2011).

In addition, HA had more sampling locations than HB with SDRD or MABE < 5% for the 1.0–2.0, and 2.0–3.0 m soil layers (relatively deeper layers), and the mean values of SDRD or MABE for the deeper layers on HA tended to be much smaller than those on HB, though the differences were not statistically significant (Table 3 and Fig. 5). The different soil moistures and vegetational covers between the two hillslopes may account for these differences. HA was relatively wetter than HB for the various soil layers (Table 2). Temporal stability in the spatial patterns of soil moisture is expected to vary between different conditions of wetness (Lin, 2006), as exhibited in this study. Our results correspond to some findings that the temporal stability of soil moisture was stronger under wet rather than dry conditions (Hupet and Vanclooster,

Table 3
Statistical summary of the mean relative difference (MRD), standard deviation of MRD (SDRD) and mean absolute bias error (MABE) in SWS for the various soil layers on HA and HB.

Parameters	HA			HB		
	0–1.0 m	1.0–2.0 m	2.0–3.0 m	0–1.0 m	1.0–2.0 m	2.0–3.0 m
MRD (%)						
Min.	−42.2	−53.5	−48.2	−32.4	−63.2	−67.2
Max.	44.1	90.4	91.4	53.4	65.3	111.7
Range	86.3	143.9	139.6	85.8	128.5	178.9
N_1	4	4	6	7	8	2
SDRD (%)						
Mean	7.4§a	4.4bc	3.3c	7.7a	5.0b	4.2bc
Min.	3.3	1.8	1.3	2.5	2.6	1.5
Max.	13.5	9.2	7.1	16.2	9.0	8.3
Range	10.2	7.4	5.8	13.7	6.4	6.8
N_2	5	23	28	5	17	20
MABE (%)						
Mean	6.2a	3.6bc	2.7c	6.2a	4.1b	3.3bc
Min.	2.0	1.7	1.0	1.8	1.9	1.3
Max.	13.1	8.4	7.1	13.0	9.4	6.4
Range	11.1	6.7	6.1	11.2	7.5	5.1
N_3	11	26	29	11	19	23

N_1, number of locations with mean relative difference ranging from −5% to +5%; N_2, number of locations with standard deviation of relative difference <5%; N_3, number of locations with mean absolute bias error <5%; and §, means followed by the same letter are not significantly different at $P < 0.05$.

2002; Zhou et al., 2007; Zhao et al., 2010). Martínez-Fernández and Ceballos (2003), however, observed contrary phenomena. A direct comparison of results among different studies, though, is difficult due to differences in the landscapes, land uses, sampling scales, and sampling times for each study (Brocca et al., 2009). Nevertheless, the relatively wetter hillslope in our study area (HA) tended to have more temporally stable locations, possibly associated with an enhanced capillary movement of water from shallower to deeper soil that thereby decreased temporal variability in deeper SWSs. Another possible cause of this result may be the strong evapotranspiration by the alfalfa on HB, which could lead to greater temporal variability in deeper SWSs.

We further strictly selected the time-stable locations as the sites with ITS and MABE values simultaneously smaller than 10% and 5%, respectively, to estimate mean SWS for the various soil layers on each hillslope. We identified 1, 5, and 10 locations for the 0–1.0, 1.0–2.0, and 2.0–3.0 m soil layers, respectively, on HA and 5, 7, and 6 sites for the respective layers on HB. HB thus had more temporally stable locations representing the hillslope mean SWS for the 0–1.0 m soil layer than did HA, perhaps due to the differences in the distributions of land use. HB was covered with homogeneous grassland, but HA had relatively more complex patterns of land use, with a mix of grassland, forest, and farmland. We further selected the time-stable locations that could be representative of two or three soil layers to accurately and effectively estimate the mean SWS for each hillslope. No single time-stable site on HA, though, was representative for all three soil depths. Location A6 was thus selected to estimate mean SWS for the 0–1.0 m soil layer, and four sites (A12, A17, A18, and A19) were deemed representative of the two deeper soil layers (i.e. 1.0–2.0, and 2.0–3.0 m). Based on its ITS values, location A19 was ultimately determined to best estimate mean SWS for the 1.0–2.0, and 2.0–3.0 m layers. In contrast to HA, a single time-stable location (B2) was found to be representative of the three soil depths on HB.

Finding a single site to represent mean SWS for all three soil layers has proven to be difficult (Vanderlinden et al., 2011). Tallon and Si (2003) found only a single representative site for two depths with low values of MRD and SDRD, and Hu et al. (2010a,b) found one representative site for five soil depths and four soil layers. Finding a single location to represent the mean SWS for several depths of large areas, though, can reduce costs while maintaining a high accuracy of prediction. To test the ability of the identified locations to accurately represent the entire hillslopes, the measured SWSs at the representative sites were plotted against the mean values for the hillslopes (Fig. 6). With a few exceptions, all sets of selected time stable locations estimate mean SWSs within 5% error at each sampling date. Linear-fitting analysis indicated that the selected representative locations directly estimated the mean SWSs well ($R^2 \geqslant 0.95$), with a relative precision of <0.001 for the various soil layers on HA (Fig. 6a) and HB (Fig. 6b), suggesting that the representative sites were appropriate for estimating hillslope mean SWS at various depths, in agreement with other studies (Jacobs et al., 2004; Guber et al., 2008; Hu et al., 2010b, 2012; Brocca et al., 2012; Gao and Shao, 2012). The present study thus demonstrated the feasibility of representing the mean SWS directly on the scale of a hillslope by measuring the soil water at a time-stable location. Schneider et al. (2008) further indicated that representative locations were appropriate for estimating mean soil moisture of the study area over multiple years. Lower values of SWS, however, were underestimated, while higher values were overestimated, by the representative sites for the 0–1.0 m soil layer, especially on HA (Fig. 6). These discrepancies may be due to the higher susceptibility of soil moisture to evapotranspiration and precipitation at the selected representative location, which may be linked to the surface properties of the selected site. Nevertheless, the identification of time-stable locations for estimating mean soil moisture of the entire study area of interest is advantageous because it can reduce the required number of samples while maintaining a high accuracy of prediction.

3.3. Factors controlling the temporal stability of soil water storage

The temporal stability of spatial patterns of soil water is related to the soil, topography, and properties of the vegetation (Mohanty and Skaggs, 2001; Jacobs et al., 2004; Cosh et al., 2008; Zhao et al., 2010). To analyse whether the MRD, and thereby temporal stability, depended on these variables, a simple correlation analysis was performed to study the dependency of temporal stability on associated parameters of the land surface. Table 4 shows the correlation between MRD and bulk density (BD), saturated soil hydraulic conductivity (Ks), clay content (Clay), sand content (Sand), organic carbon content (OC), site elevation (SE), aboveground biomass (AGB), and litter fall (Litter). The classical view of the impacts of soil, topography, and vegetation on the temporal stability of soil moisture was generally confirmed in our study area.

Our results showed that OC and SE were the most important parameters for MRD for the various soil layers on HA. The MRD, however, was correlated with BD only for the 0–1.0 m layer on HA (Table 4). In contrast, selected soil and topographic parameters, including BD, Clay, Sand, OC, and SE, were responsible for the variability of MRD for the various soil layers on HB (Table 4). We identified a substantial effect of elevation on the temporal stability of SWS, in contrast to the findings of Kaleita et al. (2004) and Zhao et al. (2010). The weak topographical effect on the temporal stability of soil water found by these authors was attributed to the relative flatness of their study area. Topography thus cannot be neglected in predicting the temporal stability of SWS spatial patterns in areas characterised by diverse or complex terrains (Grayson et al., 2002; Lin, 2006), such as those of the Loess Plateau that has a large number of deep gullies and undulating slopes. The MRD was positively correlated with both Clay and OC but negatively with BD, Sand, and SE for the various layers on HB. Similar results were also detected on HA, although poor relationships were found between the MRD and soil texture. This result was

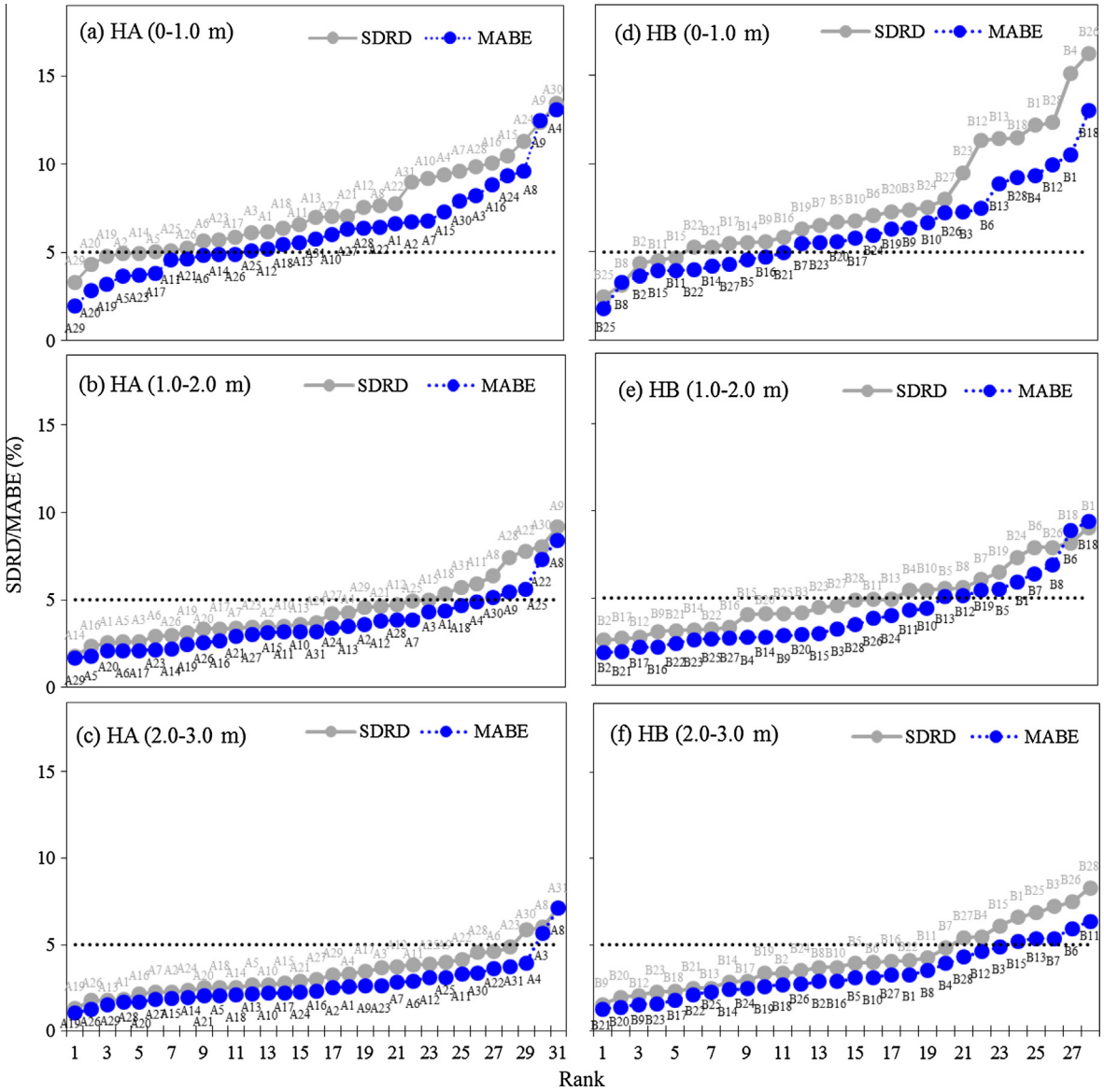

Fig. 5. Ranked standard deviation of relative differences (SDRD) and mean absolute bias error (MABE) on HA (a, b, and c) and HB (d, e, and f) for the various soil layers.

consistent with previous studies by Zhao et al. (2010) and Gao et al. (2011). All the above observations suggest the importance of soil texture, OC, and SE on the temporal stability of SWS spatial patterns on the scale of hillslopes in this study area. In addition, more soil properties on HB than on HA were found to be significantly correlated with the MRD, suggesting that the dependence of the temporally stable characteristics of sampling locations on soil properties might vary due to differences in wetness and plant covers across hillslopes.

Plant heterogeneity may also control SWS spatial patterns, because rooting structure, surface cover, and species composition affect the processes of water evapotranspiration and storage (Zhao et al., 2010). The correlation between the MRD and vegetational properties on HA cannot be further clarified due to the lack of data for AGB and Litter. The MRD was correlated with AGB and Litter on HB (Table 4). Similar to the ability of soil to retain and transmit water, the distribution of vegetation and roots can cause a highly dynamic water demand for the plants, especially for species with higher levels of evapotranspiration (e.g. alfalfa), which may complicate such correlations (Zhao et al., 2010). When vegetation strongly affects the temporal patterns of SWS during the growing season, as on HB, temporal persistence tends to be dependent on the characteristics of the vegetation (e.g. plant cover or biomass) (Schneider et al., 2008; Jia and Shao, 2013). In fact, vegetation affects soil moisture seasonally. In this study, however, the AGB was derived from a single measurement and thus did not capture the seasonal variations. We conclude that the temporal stability of SWS in the study area may be controlled by the soil, topography, and properties of the vegetation, and the effects may vary across hillslopes due to differences in wetness and plant covers.

4. Conclusions

Based on the datasets of the SWS profiles (0–3.0 m layers) collected from 59 locations on 15 monitoring occasions on the two adjacent hillslopes, the following results can be summarised:

(1) Time-averaged mean SWS for the various soil layers differed between HA and HB, mainly due to the differences in topography and vegetation.

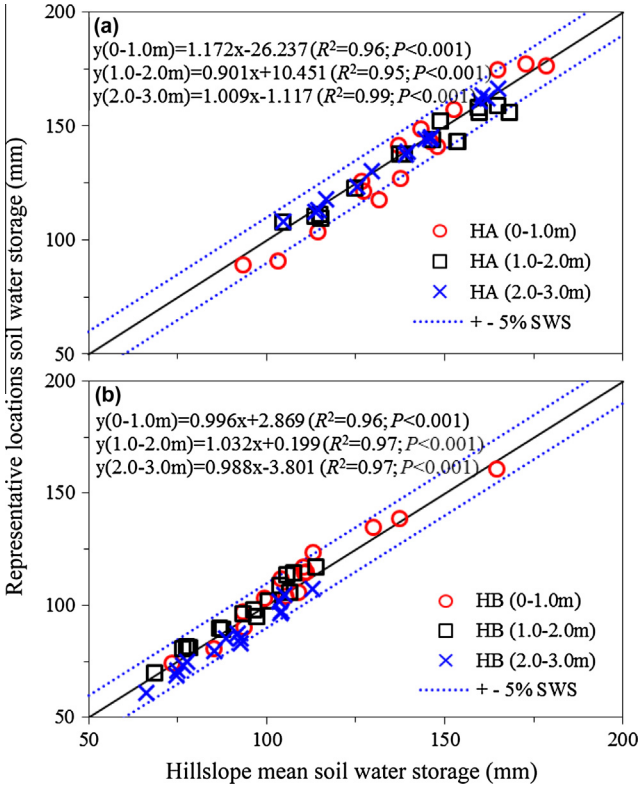

Fig. 6. Hillslope mean SWS versus the representative locations SWS for the various soil layers on HA (a) (locations A6, A19, A19 for 0–1.0, 1.0–2.0, and 2.0–3.0 m soil layers, respectively) and HB (b) (location B2 for the three soil layers) for each sampling date during the experimental period of 2009–2011.

Table 4
Pearson correlation matrix between the MRD and selected soil (bulk density, BD; saturated soil hydrologic conductivity, Ks; clay content, Clay; sand content, Sand; organic carbon content, OC), topography (site elevation, SE), and properties of the vegetation (aboveground biomass, AGB; litter fall, Litter) on HA and HB.

Parameter	HA			HB		
	0–1.0 m	1.0–2.0 m	2.0–3.0 m	0–1.0 m	1.0–2.0 m	2.0–3.0 m
Soil						
BD	−0.437*	−0.169	−0.245	−0.498**	−0.535**	−0.541**
Ks	0.204	0.021	0.052	0.174	0.174	0.010
Clay	0.258	−0.243	−0.282	0.539**	0.375*	0.529**
Sand	−0.271	0.298	0.273	−0.479**	−0.26	−0.454*
OC	0.366*	0.350*	0.357*	0.611**	0.531**	0.434**
Topography						
SE	−0.526**	−0.550**	−0.641**	−0.473*	−0.531**	−0.550**
Vegetation						
AGB	–	–	–	0.552**	0.485**	0.518**
Litter	–	–	–	0.602**	0.503**	0.605**

AGB and Litter data on the SWS sampling locations is not available on HA.
* Indicates correlation is significant at $P < 0.01$.
** Indicates correlation is significant at $P < 0.05$.

(2) Temporal changes in the mean SWS decreased with increasing soil depth, while the spatial variation increased on both hillslopes. The degree of temporal–spatial variation of SWS was strongly dependent on sampling depth.
(3) Values of SDRD and MABE for the 1.0–2.0, and 2.0–3.0 m layers were significantly lower than those for the 0–1.0 m layer. The number of time-stable locations increased with increasing soil depth on both hillslopes, indicating that the SWS tended to be more temporally stable in deeper soil.
(4) Based on the values of ITS and MABE, two and one time-stable sites were determined to be representative of the mean SWS on HA and HB, respectively, which were further verified by the high value of R^2 between the hillslope mean SWS and the representative locations SWS.
(5) Soil texture, organic carbon content, elevation, and properties of the vegetation affected the temporal stability of SWS for the various layers, but these effects differed between HA and HB, implying that the dependence of SWS temporal stability on soil, plants, and topography, on the scale of the hillslope, may differ among different hillslopes.

Future research is needed to ascertain the single and combined effects of the primary factors (e.g. measurement strategy, terrain, soils, and vegetation) in controlling SWS temporal stability, which may help to improve the rapid identification of representative sites with limited data. Finding a single representative site to estimate mean SWS at several depths for a large area can reduce the costs of measurement and save time.

Acknowledgement

This study was financially supported by the National Natural Science Foundation of China (E090103, 41271315, and 40801111), the Science and Technology Development Research Program in Shaanxi Province (2011kjxx25), and the State Key Laboratory of Soil Erosion and Dryland Farming on the Loess Plateau (K318009902-1308). Drs. L. Gao, B.X. Liu, X.Z. Li, and Y.H. Jia are acknowledged for their helps in the data collection and constructive suggestions for this paper.

References

Biswas, A., Si, B.C., 2011. Identifying scale specific controls of soil water storage in a hummocky landscape using wavelet coherency. Geoderma 165, 50–59.
Brocca, L., Melone, F., Moramarco, T., Morbidelli, R., 2009. Soil moisture temporal stability over experimental areas in Central Italy. Geoderma 148, 364–374.
Brocca, L., Melone, F., Moramarco, T., Morbidelli, R., 2010. Spatial–temporal variability of soil water and its estimation across scales. Water Resour. Res. 46, W02516. http://dx.doi.org/10.1029/2009WR008016.
Brocca, L., Tullo, T., Melone, F., Moramarco, T., Morbidelli, R., 2012. Catchment scale soil moisture spatial–temporal variability. J. Hydrol. 422–423, 63–75.
Caysi, G., Heng, L.K., Öztürk, H.S., Sürek, D., Kütük, C., Saglam, M., 2009. Crop yield and water use efficiency in semi-arid region of Turkey. Soil Till. Res. 103, 65–72.
Chanasyk, D.S., Naeth, M.A., 1996. Field measurement of soil moisture using neutron probe. Can. J. Soil Sci. 76, 317–323.
Chen, H.S., Shao, M.A., Li, Y.Y., 2008. Soil desiccation in the Loess Plateau of China. Geoderma 143, 91–100.
Choi, M., Jacobs, J.M., 2007. Soil moisture variability of root zone profiles within SMEX02 remote sensing footprints. Adv. Water Resour. 30, 883–896.
Comegna, V., Basile, A., 1994. Temporal stability of spatial patterns of soil water storage in a cultivated Vesuvian soil. Geoderma 62, 299–310.
Cosh, M.H., Jackson, T.J., Moran, S., Bindlish, R., 2008. Temporal persistence and stability of surface soil moisture in a semi-arid watershed. Remote Sens. Environ. 112, 304–313.
Gao, X.D., Wu, P.T., Zhao, X.N., Shi, Y.G., Wang, J.W., 2011. Estimating spatial mean soil water contents of sloping jujube orchards using temporal stability. Agric. Water Manage. 102, 66–73.
Gao, L., Shao, M.A., 2012. Temporal stability of soil water storage in diverse soil layers. Catena 95, 24–32.
Gómez-Plaza, A., Alvarez-Rogel, J., Albaladejo, J., 2000. Spatial patterns and temporal stability of soil moisture across a range of scales in a semi-arid environment. Hydrol. Process. 14, 1261–1277.
Grayson, R.B., Western, A.W., 1998. Towards areal estimation of soil water content from point measurements: time and space stability of mean response. J. Hydrol. 207, 68–82.
Grayson, R.B., Blöschl, G., Western, A.W., McMahon, T.A., 2002. Advances in the use of observed spatial patterns of catchment hydrological response. Adv. Water Resour. 25, 1313–1334.
Guber, A.K., Gish, T.J., Pachepsky, Y.A., van Genuchten, M.T., Daughtry, C.S.T., Nicholson, T.J., Cady, R.E., 2008. Temporal stability in soil water content patterns across agricultural field. Catena 73, 125–133.
Heathman, G.C., Larose, M., Cosh, M.H., Bindlish, R., 2009. Surface and profile soil water spatio-temporal analysis during an excessive rainfall period in the Southern Great Plains, USA. Catena 78, 159–169.

Hu, W., Shao, M.A., Wang, Q.J., Reichardt, K., 2009. Time stability of soil water storage measured by neutron probe and the effects of calibration procedures in a small watershed. Catena 79, 72–82.
Hu, W., Shao, M.A., Han, F.P., Reichardt, K., Tan, J., 2010a. Watershed scale temporal stability of soil water content. Geoderma 162, 260–272.
Hu, W., Shao, M.A., Reichardt, K., 2010b. Using a new criterion to identify sites for mean soil water storage evaluation. Soil Sci. Soc. Am. J. 74, 762–773.
Hu, W., Tallon, L.K., Si, B.C., 2012. Evaluation of time stability indices for soil water storage upscaling. J. Hydrol. 475, 229–241.
Hupet, F., Vanclooster, M., 2002. Intraseasonal dynamics of soil moisture variability within a small agricultural maize cropped field. J. Hydrol. 261, 86–101.
Jacobs, J.M., Mohanty, B.P., Hsu, E.C., Miller, D., 2004. SME02: field scale variability, time stability and similarity of soil moisture. Remote Sens. Environ. 92, 436–446.
Jia, Y.H., Shao, M.A., 2013. Temporal stability of soil water storage under four types of revegetation on the northern Loess Plateau of China. Agric. Water Manage. 117, 33–42.
Kachanoski, R.G., de Jong, E., 1988. Scale dependence and the temporal stability of spatial patterns of soil water storage. Water Resour. Res. 24, 85–91.
Kaleita, A.L., Tian, L.F., Hirschi, M.C., 2004. Identification of optimal sampling locations and grid size for soil moisture mapping. ASAE Paper No.041146. http://asae.frymulti.com/azdez.asp?JID=5&AID=16171&CID=can2004&T=2 (accessed 13 September. 2012).
Kirda, C., Reichardt, K., 1992. Comparison of neutron moisture gauges with nonnuclear methods to measure field soil water status. Sci. Agric. Piracicaba-SP 49, 111–121.
Klute, A., Dirksen, C., 1986. Hydraulic conductivity of saturated soils. In: Klute, A. (Ed.), Methods of Soil Analysis. ASA and SSSA, Madison, Wisconsin, USA, pp. 694–700.
Lin, H., 2006. Temporal stability of soil water spatial pattern and subsurface preferential flow pathways in the shale hills catchment. Vadose Zone J. 5, 317–340.
Martínez-Fernández, J., Ceballos, A., 2003. Temporal stability of soil moisture in a large-field experiment in Spain. Soil Sci. Soc. Am. J. 67, 1647–1656.
Martínez-Fernández, J., Ceballos, A., 2005. Mean soil moisture estimation using temporal stability analysis. J. Hydrol. 312, 28–38.
Mohanty, B.P., Skaggs, T.H., 2001. Spatio-temporal evolution and time-stable characteristics of soil moisture within remote sensing footprints with varying soil, slope, and vegetation. Adv. Water Resour. 24, 1051–1067.
Muñoz-Carpena, R., 2012. Field devices for monitoring soil water content. Agricultural and Biological Engineering Department, University of Florida. BUL343. <http://edis.ifas.ufl.edu>.
Nelson, D.W., Sommers, L.E., 1982. Total carbon, organic carbon and organic matter. In: Page, A.L., Miller, R.H., Keeney, D.R. (Eds.), Methods of Soil Analysis. Part 2. Agronomy Monograph, second ed. ASA and SSSA, Madison, WI, pp. 534–580.
Pachepsky, Ya., Guber, A., Jacques, D., 2005. Temporal persistence in vertical distribution of soil moisture contents. Soil Sci. Soc. Am. J. 69, 347–352.
Penna, D., Brocca, L., Borga, M., Fontana, D.G., 2013. Soil moisture temporal stability at different depths on two alpine hillslopes during wet and dry periods. J. Hydrol. 477, 55–71.
Reichardt, K., Portezan-Filho, O., Bacchi, O.O.S., Oliveira, J.C.M., Dourado-Neto, D., Pilotto, J.E., Calvache, M., 1997. Neutron probe calibration correction by temporal stability parameters of soil water content probability distribution. Sci. Agric. 54, 17–21.
Schneider, K., Huisman, J.A., Breuer, L., Zhao, Y., Frede, H.-G., 2008. Temporal stability of soil moisture in various semi-arid steppe ecosystems and its application in remote sensing. J. Hydrol. 359, 16–29.
Starks, P.J., Heathman, G.C., Jackson, T.J., Cosh, M.H., 2006. Temporal stability of soil moisture profile. J. Hydrol. 324, 400–411.
Tallon, L., Si, B.C., 2003. Representative soil water benchmarking for environmental monitoring. J. Environ. Inform. 4, 28–36.
Vachaud, G., Passerat de Silans, A., Balabanis, P., Vauclin, M., 1985. Temporal stability of spatially measured soil water probability density function. Soil Sci. Soc. Am. J. 49, 822–828.
Vanderlinden, K., Vereecken, H., Hardelauf, H., Herbst, M., Martínez, G., Cosh, M.H., Pachepsky, Y.A., 2011. Temporal stability of soil water contents: a review of data and analyses. Vadose Zone J. http://dx.doi.org/10.2136/vzj2011.0178.
Wang, Y.Q., Shao, M.A., Shao, H.B., 2010. A preliminary investigation of the dynamic characteristics of dried soil layers in the Loess Plateau of China. J. Hydrol. 381, 9–17.
Wang, Y.Q., Shao, M.A., Liu, Z.P., Warrington, D.N., 2012. Regional spatial pattern of deep soil water content and its influencing factors. Hydrol. Sci. J. 57, 265–281.
Western, A.W., Zhou, S.L., Grayson, R.B., McMahon, T.A., Blöschl, G., Wilson, D.J., 2004. Spatial correlation of soil moisture in small catchments and its relationship to dominant spatial hydrological processes. J. Hydrol. 286, 113–134.
Xia, Y.Q., Shao, M.A., 2008. Soil water carrying capacity for vegetation: a hydrologic and biogeochemical process model solution. Ecol. Model. 214, 112–124.
Zhao, Y., Peth, S., Wang, X.Y., Lin, H., Horn, R., 2010. Controls of surface soil moisture spatial patterns and their temporal stability in a semi-arid steppe. Hydrol. Process. 24, 2507–2519.
Zhou, X., Lin, H., Zhu, Q., 2007. Temporal stability of soil moisture spatial variability at two scales and its implication for optimal field monitoring. Hydrol. Earth Syst. Sci. Discuss. 4, 1185–1214.